

# Modeling of a two-step solar hydrogen production plant

Alberto de la Calle<sup>a,\*</sup>, Lidia Roca<sup>a</sup>, Luis J. Yebra<sup>a</sup>, Sebastián Dormido<sup>b</sup>

<sup>a</sup>*CIEMAT - Plataforma Solar de Almería, Ctra. De Senés s/n 04200 Tabernas, Spain*

<sup>b</sup>*UNED, Escuela Técnica Superior de Ingeniería Informática, 28040 Madrid, Spain*

---

## Abstract

The promising advances in the research of two-step solar hydrogen production from water have increased the interest in producing hydrogen with this technology. In this framework, Hydrosol II Project pilot plant was set up at CIEMAT - Plataforma Solar de Almería with the aim of producing continuous solar hydrogen from water **based on a ferrite-based redox technology**. The process switches sequentially oxidation and reduction steps with a operational temperatures of 800 and 1200 °C obtaining a quasi-continuous hydrogen production working in parallel two reactors.

A dynamic model of a solar hydrogen production plant has been developed based on the experience of this pilot plant. It have been designed to be a platform to test control algorithms to automate the hydrogen production. The new model includes a solar field model and a process plant model and it is able to simulate the concentrated solar power received on the reactors and the thermal and chemical behaviour of the reactors. The solar field model and the plant thermal behaviour has been calibrated and validated

---

\*Corresponding author. Tel.: +34 950 387964; Fax: +34 950 365015

*Email addresses:* [alberto.calle@psa.es](mailto:alberto.calle@psa.es) (Alberto de la Calle), [lidia.roca@psa.es](mailto:lidia.roca@psa.es) (Lidia Roca), [luis.yebra@psa.es](mailto:luis.yebra@psa.es) (Luis J. Yebra), [sdormido@dia.uned.es](mailto:sdormido@dia.uned.es) (Sebastián Dormido)

with experimental data. The numerical predictions show a good agreement with measurement data.

*Keywords:*

solar hydrogen, water splitting, model, calibration, Modelica

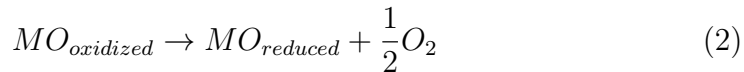
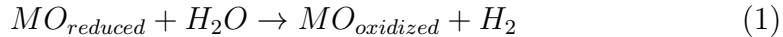
---

## 1. Introduction

In the research of new clean alternative energies, the technologies related to hydrogen have achieved a good position as a result of its potential to replace fossil fuels in numerous applications. This is the reason why researches on new ways of hydrogen production have been intensified [1]. Due to its abundance and affordability, water is the ideal raw material to produce hydrogen. The water splitting process using only heat (water thermolysis) requires very high temperatures (above 2500 K) to achieve some significant degree of dissociation and the technique needed to separate this highly explosive mixture is expensive [2]. Water splitting thermochemical cycles are one of the most promising techniques to achieve the dissociation bypassing the separation and the high temperature problem. This kind of systems have the advantage of requiring much lower temperatures, which are attainable with concentration solar systems. Furthermore, a complex separation technique is not necessary because the hydrogen and oxygen are produced in different steps. In [2], [3], [4] and [5] reviews of thermo-chemical cycles of solar hydrogen production are given.

Two-steps redox systems has been studied as one of the more efficient water splitting thermochemical cycles [2]. The metal oxides which are reduced have a high capacity to absorb oxygen from water. The two-step redox sys-

tems use this property to release the hydrogen. On the first step (water splitting), a reduced metal oxide absorbs the oxygen from the water producing hydrogen (1). On the second step (regeneration), the oxide is reduced again, releasing the absorbed oxygen during the water splitting (2).



In the Hydrosol project, the continuous solar hydrogen production from water based on these ideas has been developed and demonstrated in [6]. The aim of Hydrosol II project was to develop a feasibility study for a large-scale production plant. As a results of this study a pilot plant was set up at CIEMAT - Plataforma Solar de Almería [7]. The data contained in this paper belongs to Hydrosol 3D project whose goal is to carry out a feasibility study for a commercial-scale production plant.

In [6] was presented a model of the first laboratory reactor built in the framework of Hydrosol project. The model was able to predict the thermal dynamics of the reactor using a radial finite volume method to calculate mass and energy balances. It was validated with experimental data using the solar flux from a solar furnace where the flux distribution in the absorber was less homogeneous than one from a central receiver system.

A new system model of a hydrogen production process was presented in [8]. This system model consists in three blocks interconnected through a model control software which manages the communications between them and the inputs and outputs using a **Labview<sup>®</sup>** interface. The three block

are: a flux distribution simulation tool, a temperature model and a hydrogen production model. The flux distribution simulation tool is a modular ray tracing code developed in c-language and assembler language and embedded in a Labview<sup>®</sup> interface which simulates the flux distribution calculating the number of rays which strike per unit area the reactor module aperture using deflectometry measurements of representative heliostats which evaluate the local slope of the mirror through the study of the deformations in a stripe pattern reflected on the heliostat surface [9]. The temperature and the hydrogen production models are programmed in the Labview<sup>®</sup> simulation module. The hydrogen production model uses a Shrinking Core Model which was fitted with empirical data in [10].

The present paper proposes, describes and develops a new dynamic model of a hydrogen production plant based on the Hydrosol II facilities. It models the whole process of hydrogen production, so it includes the heliostat field and the process plant where the reactors are. It has been developed with the aim of testing control algorithms which make possible an automatic hydrogen production. Its low computational effort allows a fast simulation of hydrogen production for control tests. Besides, it can be also used to study the behaviour of the production plant in several scenarios and with different operational strategies to optimize the future strategies of operational control. The object-oriented modeling language Modelica allows us to develop a non-linear first-principles model and the solar field model and the plant thermal behaviour has been calibrated using the Matlab<sup>®</sup>'s Global Optimization Toolbox. These behaviours have been validated with experimental results obtained in the Hydrosol pilot plant. This model can be used in a real-time

simulation if it is assembled in a Labview<sup>®</sup> interface which provides model inputs.

The proposed model will be a powerful tool to test control algorithms such as focusing the heliostats of the solar field on each receiver to reach the desired temperatures in both reactors. Notice the heliostat operation's strategy is a manual one, based on the operators' wide experience. Although the results obtained with this strategy are enough to operate in nominal conditions, an automatic control would improve the operation dealing with disturbances, such as the variable solar irradiance.

## 2. System description

The pilot plant for solar hydrogen production was set up at CIEMAT - Plataforma Solar de Almería with a maximum power of 100 kW<sub>th</sub> [7]. It consist in two reactors where the reactions are alternated in cycles of hydrogen and oxygen production. As a result, there is a continuous hydrogen production. The thermal power achieved must be different in each cycle because different amount of power are required in each reaction. The water splitting step (1) is a exothermic reaction and the operating temperature is  $T_{gen} = 800$  °C. The thermal reduction step (2) is a endothermic reaction and the operating temperature is  $T_{reg} = 1200$  °C. In order to be produced, reactions require a gaseous atmosphere, that is, a mixture of nitrogen and steam in the generation cycle and just nitrogen in regeneration cycle. The nitrogen is used as an inert gas to push the reaction products.

From a dynamic system point of view the plant, whose diagram is showed in Fig. 1, could be analyzed as follows. Each reactor receives only one inlet

flow controlled by MV1 and MV2 valves. One inlet flow is  $N_2$  and the other  $H_2O-N_2$ . The  $N_2$  is heated up by H0 or H1 heater depending on the branch. The  $H_2O-N_2$  mixed flow is heated up by H2 heater and it must be controlled in volume and in composition by FC2 and FC3 valves. For the reaction to take place, a controlled amount of power must arrive at the aperture of the receiver. This power comes from a solar heliostat field.

The reactors are installed in SSPS-CRS facility at CIEMAT - Plataforma Solar of Almería (see Fig. 2). Under typical conditions of  $950 \text{ W/m}^2$ , the total field capacity is  $2.7 \text{ MW}_{th}$  and the peak flux is  $2.5 \text{ MW/m}^2$ . Approximately the 99% of the power is collected in a 2.5 m-diameter circumference and 90% in a 1.8 m circumference. **The reactor aperture has a size of 0.5 m x 0.5 m therefore not all of the power get to the reactor's absorber through a quartz glass window but this power has density almost homogeneous.** The reactor's absorber is made of nine honeycomb monoliths, **each with a size of 0.146 m x 0.146 m x 0.06 m**, that are assembled as one single module. The monoliths are made of silicon carbide (SiC) and they are used as **substrate** for the oxides needed for the reactions. The gas flows inside the reactor through the channels of the monoliths and there is where the reaction takes place.

### 3. Object-oriented modeling

The model has been developed in Modelica language [11]. This language allows to formulate the problems in an acausal way, therefore, the translation of the physical equations to the formulation language is direct, being very well suited for representing the physical structure of modeled systems [12]. Modelica is also an object-oriented language which provide the encapsulation

through classes. The abstraction which can be obtained with this kind of languages makes easier to divide the problem in modules that can be re-used. Using this characteristic the model presented in this paper has been divided in two interconnected models, the heliostat field model and the process plant model. This relationship is showed in Fig. 3.

### *3.1. Simplified solar field model*

Heliostats reflect solar radiation and concentrate it in the aperture of both receivers.

Several algorithms are available to calculate this solar flux concentration and its distribution on the central receiver. As explained [13], two categories may be distinguished regarding to flux calculation algorithms. The first one includes software to design solar plants to maximize the collected solar energy, whereas the second category includes codes for evaluating the power reflected by the heliostats and which gets in the receiver. Since these algorithms are designed to obtain high degree of precision, the numerical model may be too complex with a high computational effort to be used in real-time applications. In [9] a new software to calculate the flux density distribution reducing **the MIRVAL's computation time [14] in 6 is developed. Despite this, the software is slow to be considerate in real-time simulations.**

A simplified solar field model has been developed to estimate the flux concentration in the receivers of Hydrosol facility. **Model was developed assuming losses in the accuracy but reducing the computational effort as much as it has been possible, making the model works in real-time simulations.** To reduce the complexity of the model, the following hypotheses have been assumed:

- tracking errors are neglected,
- the flux density is homogeneous on the receiver plane,
- slope, shading and blocking errors are assumed to be constants.

Due to the aperture is small (see section 2) in comparative with the Gaussian slope flux density only a part near the peak through the aperture. This flux density distribution that gets the absorber is almost homogeneous and this effect is increased with the neglected small errors in heliostats focusing.

Then, the flux generated by the  $k$ -heliostat,  $f_k$ , may be approximated as:

$$f_k = I \cdot \cos(\alpha_{ik}) \cdot A_h \cdot \beta \cdot (1 - \gamma) \quad (3)$$

and the flux concentrated in the receiver,  $F$ , is:

$$F = \sum_{k=1}^{n_t} f_k \quad (4)$$

where  $n_t$  is the number of heliostats in the field,  $I$  is the direct solar irradiance,  $\alpha_i$  is the solar vector incident angle in the heliostat plane,  $A_h$  is the heliostat mirror area,  $\beta$  is a parameter which includes slope, shading and blocking errors and the optical efficiency of the heliostats and  $\gamma$  is the atmospheric attenuation factor. Notice that the incident angle depends on the Sun position,  $P_s=(s_x, s_y, s_z)$ , and on the azimuth and elevation angles of each heliostat,  $\alpha_a, \alpha_e$ :

$$\alpha_{ik} = f(P_s, \alpha_{ak}, \alpha_{ek}) \quad (5)$$

The parameter  $\beta$ , it is assumed to be single and constant for all the heliostats. This is a fitting parameter and needs to be calibrated. The

atmospheric attenuation factor is the same used in MIRVAL code for a clear day [14]:

$$\gamma = 10^{-4}(67.9 + 1.179s - 1.9710^{-4}s^2) \quad (6)$$

where  $s$  is the slant range from the heliostat to the receiver and must be less than one kilometre.

Since the model must be as simple as possible, it is assumed that there are no tracking errors so that the ray reflected from the mass center of the heliostat mirror reaches the target on the receiver. Moreover it is supposed that the flux density is homogeneous on the receiver plane. Therefore,  $\alpha_i$  it is obtained as a function of the Sun position, the coordinates of each heliostat,  $P_h=(h_x, h_y, h_z)$ , and the target receiver focus,  $P_t=(t_x, t_y, t_z)$ :

$$\alpha_{ik} = f(P_s, P_{hk}, P_t) \quad (7)$$

To determine the coordinates of the Sun, the algorithm proposed in [15] is used.

### 3.2. Process plant model

In order to have a low computational effort model, the mathematical model was developed trying to minimize the number of equations but keeping the essential principles.

One of the main assumptions is that the  $N_2$  and  $H_2O$  lines, which feed the reactors, have been modeled as two flow sources. These flow sources provide constant mass flows at fixed temperatures of 200 °C and atmospheric pressure. The two flow sources switch between each other like the cycles, providing a  $N_2$  or a  $H_2O - N_2$  flow.

The reactor has been modeled as a single mass block which exchanges energy with convective and radiative processes between the environment and the gas inside the reactor, neglecting conduction heat exchanger because of its low contribution. Moreover, we have also neglected the conduction process inside the mass block assuming that the block has a single temperature. The specific heat capacity of this mass block and the heat transfer coefficients **are assumed as constants** parameters to be calibrated with real data as it is explained in section 4. The energy balance equations are:

$$U_{reac} = m_{reac}C_{reac}T_{reac} \quad (8)$$

$$\dot{U}_{reac} = \dot{Q}_{helio} - \dot{Q}_{conv,gas} - \dot{Q}_{rad,env} - \dot{Q}_{conv,env}$$

where  $U_{reac}$  is the reactor's internal energy,  $m_{reac}$  the reactor's mass,  $T_{reac}$  the reactor's temperature.  $\dot{Q}_{helio}$  is the heat flow resulting from the heliostat field,  $\dot{Q}_{conv,gas}$  the transfer heat with the gas inside the reactor and  $\dot{Q}_{conv,env}$  and  $\dot{Q}_{rad,env}$  the heat losses between the reactor and the environment. Its expressions are:

$$\dot{Q}_{conv,gas} = H_{conv,gas}(T_{reac} - T_{gas}) \quad (9)$$

$$\dot{Q}_{conv,env} = H_{conv,env}(T_{reac} - T_{env}) \quad (10)$$

$$\dot{Q}_{rad,env} = H_{rad,env}(T_{reac}^4 - T_{gas}^4) \quad (11)$$

The energy balance inside the reactor is only modeled as the mixture gas energy balance. Neglecting the energy consumed by the reaction, the equation is a balance between the convection heat received and the work

done by the gas and the negative balance given by the cold inlet gas and the hot outlet gas, such as:

$$U_{gas} = m_{gas}C_{gas}T_{gas} - p_{gas}V \quad (12)$$

$$\dot{U}_{gas} = \dot{Q}_{conv,gas} + \dot{m}_{gas,in}C_{gas}T_{gas,in} - \dot{m}_{gas,out}C_{gas}T_{gas,out}$$

where  $m_{gas}$  is the sum of the masses of different gases. The reactor pressure,  $p_{gas}$ , is calculated with a Van der Waals equation of state because at high temperatures its performance is better than the one obtained by the ideal gas law. It is considered only one specific capacity **assumed as constant parameter to be calibrated** because including particular specific capacities, for each gas in the mixture inside the reactor, adds **an unnecessary complexity to the model. This is possible due to the specific capacities of this gases are in the same order of magnitude and the low gas mass inside the reactor.**

To properly calculate the gas mass balance, the reactions that take place inside the reactor must be included. For this reason it is more appropriate to define the system with a molar balance where the moles,  $n$ , will be calculated according to the reaction kinetics. The reaction rates are assumed to be those included in [16]:

$$R_{gen} = k_{gen}n_M n_{H_2O} \quad (13)$$

$$R_{reg} = k_{reg}n_{MO} \quad (14)$$

where reaction rate constants,  $k_{gen}$  and  $k_{reg}$ , have an Arrhenius dependence.

$$k = k_0 e^{-E_0/RT} \quad (15)$$

and where  $n_M$  and  $n_{MO}$  are not the total moles of these elements in the reactors, metal oxide reduced and metal oxide respectively, but the available ones because only a fraction of the oxide in the surface has the ability to be reduced. Its sum is assumed to be constant and it **will be calibrated with real data in future experiments**.

With these reaction rates (13, 14) the molar balance inside the reactor is as follows:

$$\dot{n}_M = R_{reg} - R_{gen} \quad (16)$$

$$\dot{n}_{H_2O} = -R_{gen} + \dot{n}_{H_2O,in} - \dot{n}_{H_2O,out} \quad (17)$$

$$\dot{n}_{MO} = R_{gen} - R_{reg} \quad (18)$$

$$\dot{n}_{H_2} = R_{gen} - \dot{n}_{H_2,out} \quad (19)$$

$$\dot{n}_{O_2} = R_{reg} - \dot{n}_{O_2,out} \quad (20)$$

$$\dot{n}_{N_2} = \dot{n}_{N_2,in} - \dot{n}_{N_2,out} \quad (21)$$

The gas leaves the reactors through an orifice which connects the reactors to the escape pipe to the environment. To model the outlet flow, the Bernoulli's principle is used, assuming that it is valid with compressible fluids (gases) moving at low **Mach** numbers, where the sum of all forms of mechanical energy in a fluid along a streamline is the same in all the points on that streamline, such as:

$$p + \rho gz + \frac{\rho v^2}{2} = constant \quad (22)$$

where  $\rho$  is the fluid density,  $g$  the gravity,  $z$  the elevation over a reference point and  $v$  the flow **velocity**.

The two points of the streamline are distributed as follows: one of the points is located inside the reactor but outside the orifice and the other inside

the orifice at the same elevation. The flow rate inside the orifice is rejected because the area of the reactor is much bigger than the area of the orifice. The outlet flow **velocity** is:

$$v = [2(p_{gas} - p_{env})\rho^{-1}]^{1/2} \quad (23)$$

The outlet flow is calculated using the following expression:

$$\dot{m}_{gas,out} = C_d A_o v \rho \quad (24)$$

where  $C_d$  is the coefficient of discharge which shows us a relationship between the real and the theoretic flow and  $A_o$  is the orifice's area. These two parameters only appear in the equation (24) and they are multiplying. Therefore they are calibrated as one single parameter.

#### 4. Model calibration

The calibration of the model was made using experimental series from Hydrosol 3D project. **In these series there is no reliable information about the concentration of the outlet gas because of the high degradation grade of the oxide. The fitting parameters related to the reaction kinetics, activation energies and rate constants were not calibrated, they were taken from [16].** Due to in this pilot plant there have been tested oxides with different compositions the chemical fitting parameters are not as relevant as solar field fitting parameters or thermal fitting parameters because they always must be same in the all the experimental scenarios. In the solar field model de only parameter to be calibrated is  $\beta$ . The thermal fitting parameters are the specific heat capacities, the heat transfer coefficients, the Van der Waals equation of state constants and the coefficient of discharge.

To reduce the complexity of the calibration, solar field model and process plant model has been calibrated separately. Despite this, the complexity of the equation system of the models made that a calibration using analytical methods had been rejected. In his stead, an heuristic method was chosen in spite of this methods can not assure find the optimal solution.

Combining Modelica Library with Matlab<sup>®</sup> makes easier the calibration of the model with the measurements [17] [18]. The simulation tools used are Dymola<sup>®</sup> (to manage the Modelica Language) and Matlab<sup>®</sup> with the Global Optimization Toolbox and Simulink<sup>®</sup>. The Matlab<sup>®</sup>'s Global Optimization Toolbox lets find a near optimal tuning of the parameters.

The genetic algorithm selected determines how good the adjustment will be and how many time the calibration will need. With the aim of reducing the calibration time, the unknown parameters are firstly tuned manually. Then, one individual with a good fitness is added to the initial population. Moreover, the value ranges have been constrained to the possible ones. With these improvements, only 20 individuals and 50 generations were needed to obtain the optimal fitness for the thermal fitting parameters.

The solar field fitting parameter,  $\beta$ , has been calibrated using as a objective function the absolute error between the concentrated solar power measure and the simulated one.

Since some of the thermal fitting parameters which were calibrated only affect to specific outputs, two objective functions were used. The absolute error in the reactor's temperature is one of the objective functions because of the sensitivity of the reactions with the reaction's temperature (in the model the reaction's temperature is equals to the reactor's temperature).

The second objective function is the absolute error in the gas temperature because both are related to the heat transfer processes. As result of this optimization problem a set of solutions with the same Pareto efficiency are obtained. The chosen solution was the one that has the best balance between the two objective functions.

## 5. Results

In order to validate the model, the simulation results have been compared with a series of real data experiments from Hydrosol II pilot plant. Since it is a first-principles model, it could be shown all of the variables used in the model (e.g temperatures, heat transfer rates, outlet mass flow, concentrations, pressures, reaction rates, numbers of mole...). But, the most important variables in our purposes are the total flux concentration in the reactor because it is the input of the process plant model and the reactor and the gas temperatures because the sensitivity of the reactions with the reaction's temperature.

One day of the experimental data series used to validate the model are shown in Fig. 4 and Fig. 5. At the first, real inputs from the pilot plant used in the model (irradiance and number of heliostats focused) are represented whereas, at the second, the outputs of the model and the real data (total flux concentration, reactor's temperature and gas temperature) are presented. At the top of Fig. 5, it is shown the power concentrated in one reactor, the experimental value of that measure is obtained with a rotational moving bar with a lambertian target and a CCD camera to capture the irradiance distribution [19]. This measurement has an error percentage of at least  $\pm 3\%$ .

At the bottom a comparison between the real and simulated reactor and gas temperatures can be observed. The reactor in the absorber has one thermocouple for each monolith, therefore the temperature used in this comparison is an average temperature of all the monoliths. Both the thermocouple and the input device have an error percentage **in the temperature measurement of at least  $\pm 5\%$** . In this figure it can be observed that the model follows quite well the real behaviour of the system. The model tracks the real data in the whole curve, in the start-up as well as in the generation and regeneration steps, demonstrating the validity of the dynamic model. The absolute error was  $\pm 19.91$  K and  $\pm 15.06$  K and the relative error 1.51% and 1.33% for the reactor and the gas temperatures respectively.

It is important to emphasize that since the model has two partial models and one of them uses the results from the other one, in the second one the error is accumulated and it has a great dependence on the first model error. This dependence is demonstrated in Fig. 6 where the error between the simulated and the measured concentrated power was higher than in the day shown in Fig. 5, **at the start because the focus was not correctly centered on the aperture, and then, probably due to the heliostat surface dirtiness**. This uncertainty is necessarily propagated to the process plant model and, as a consequence, the error between the simulated and the real temperatures increases.

## 6. Conclusions

A new dynamic model of a two-step solar hydrogen production plant has been developed. This **non-linear** model is based on physical principles

and it predicts the thermal and chemical behaviour of a production plant including the heliostat field and the process plant. The model has been done in Modelica language and it has been calibrated by genetic algorithms using the **Matlab**<sup>®</sup>'s Global Optimization Toolbox. The validation of the thermal behaviour of the model has been carried out using experimental series of Hydrosol pilot plant obtaining successful results.

The low computational effort of the model developed allows to use this model to test control algorithms with the aim of making the hydrogen production automatic. The current manual heliostat operation strategy will be improved by an automatic control developed using this model. The aim is to control the temperature in both reactors despite any possible disturbances such as solar irradiance.

The next steps of the work will be on one hand to calibrate and validate the chemical behaviour of the model with experiments obtained in next experimental campaigns, in the other to develop a control system that will be able to follow a wanted thermal behaviour.

## **Acknowledgements**

The authors would like to thank the European Commission for co-funding of this work within the Project HYDROSOL-3D "Scale Up of Thermochemical Hydrogen Production in a Solar Monolithic Reactor: a 3<sup>rd</sup> Generation Design Study (Call GCH-JU-2008-1, Activity SP1-JTI-FCH-2.3: Water decomposition with solar heat sources, Project Number 2425224). Besides, the authors would like to thank the CIEMAT Research Centre and the Spanish Ministry of Science and Innovation for funding the project DPI2010-21589-

C05-02.

- [1] Pregger, T., Graf, D., Krewitt, W., Sattler, C., Roeb, M., Möller, S.. Prospects of solar thermal hydrogen production processes. *Int J Hydrogen Energy* 2009;34:4256 – 4267.
- [2] Steinfeld, A.. Solar thermochemical production of hydrogen—a review. *Sol Energy* 2005;78:603 – 615.
- [3] Serpone, N., Lawless, D., Terzian, R.. Solar fuels: Status and perspectives. *Sol Energy* 1992;49:221 – 234.
- [4] Funk, J.. Thermochemical hydrogen production: past and present. *Int J Hydrogen Energy* 2001;26:185 – 190.
- [5] Kodama, T., Gokon, N.. Thermochemical cycles for high-temperature solar hydrogen production. *Chem Rev* 2007;107:4048–4077.
- [6] Roeb, M., Neises, M., Säck, J., Rietbrock, P., Monnerie, N., Dersch, J., et al. Operational strategy of a two-step thermochemical process for solar hydrogen production. *Int J Hydrogen Energy* 2009;34:4537–4545.
- [7] Roeb, M., Säck, J.P., Rietbrock, P., Prahl, C., Schreiber, H., Neises, M., et al. Test operation of a 100kw pilot plant for solar hydrogen production from water on a solar tower. *Sol Energy* 2011;85:634 – 644.
- [8] Säck, J.P., Roeb, M., Sattler, C., Pitz-Paal, R., Heinzl, A.. Development of a system model for a hydrogen production process on a solar tower. *Sol Energy* 2011;:-.

- [9] Belhomme, B., Pitz-Paal, R., Schwarzbözl, P., Ulmer, S.. A new fast ray tracing tool for high-precision simulation of heliostat fields. *J Sol Energ- T ASME* 2009;131:031002.
- [10] Neises, M., Roeb, M., Schmücker, M., Sattler, C., Pitz-Paal, R.. Kinetic investigations of the hydrogen production step of a thermochemical cycle using mixed iron oxides coated on ceramic substrates. *Int J Energ Res* 2010;34:651–661.
- [11] Modelica Association, . Modelica specification 2.2.1. 2007.
- [12] Fritzson, P.. Principles of object-oriented modeling and simulation with Modelica 2.1. Wiley-IEEE Press; 2004.
- [13] Garcia, P., Ferriere, A., Beziau, J.. Codes for solar flux calculation dedicated to central receiver system applications: A comparative review. *Sol Energy* 2008;82:189–197.
- [14] Leary, P., Hankins, J.. User’s guide for MIRVAL: A computer code for comparing designs of heliostat-receiver optics for central receiver solar power plants. Tech. Rep. SAND77-8280; 1979.
- [15] Blanco-Muriel, M., Alarcón-Padilla, D., López-Moratalla, T., Lara-Coira, M.. Computing the solar vector. *Sol Energy* 2001;70:431–441.
- [16] Agrafiotis, C.C., Pagkoura, C., Lorentzou, S., Kostoglou, M., Konstandopoulos, A.G.. Hydrogen production in solar reactors. *Catal Today* 2007;127:265 – 277.

- [17] Hongesombut, K., Mitani, Y., Tsuji, K.. An incorporated use of genetic algorithm and a modelica library for simultaneous tuning of power system stabilizers. In: Proceedings of the 2nd International Modelica Conference. 2002, p. 89–98.
- [18] Bonilla, J., Yebra, L.J., Dormido, S., Zarza, E.. Parabolic-trough solar thermal power plant simulation scheme, multi-objective genetic algorithm calibration and validation. *Sol Energy* 2012;86:531–540.
- [19] Ballestrín, J., Monterreal, R.. Hybrid heat flux measurement system for solar central receiver evaluation. *Energy* 2004;29:915–924.

**List of Figures**

1	Hydrosol II project pilot plant flow sheet . . . . .	21
2	Hydrosol II project pilot plant at CIEMAT - Plataforma Solar de Almería during operation . . . . .	22
3	Model diagram . . . . .	23
4	Inputs to the model to validate the thermal behaviour . . . . .	24
5	Validation of the thermal behavior of the model with experimental data . . . . .	25
6	An example of the dependence between the two partial models	26

**List of Tables**

1	Variables list . . . . .	27
2	Subscripts list . . . . .	29

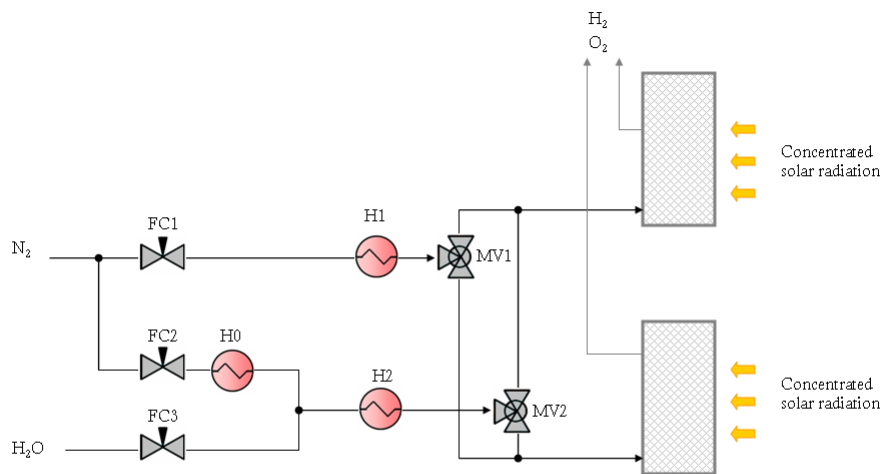


Figure 1: Hydrosol II project pilot plant flow sheet



Figure 2: Hydrosol II project pilot plant at CIEMAT - Plataforma Solar de Almería during operation

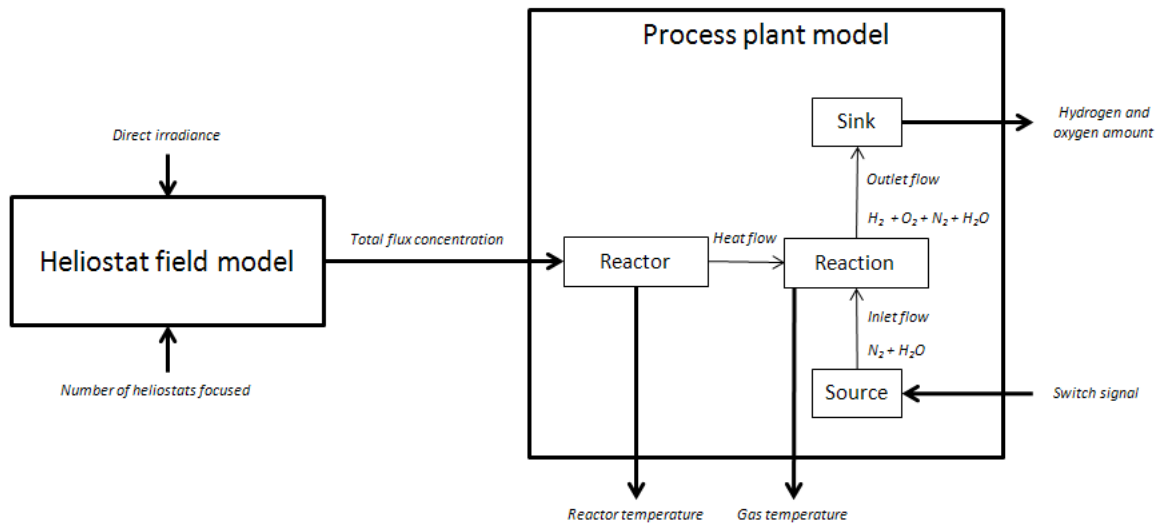


Figure 3: Model diagram

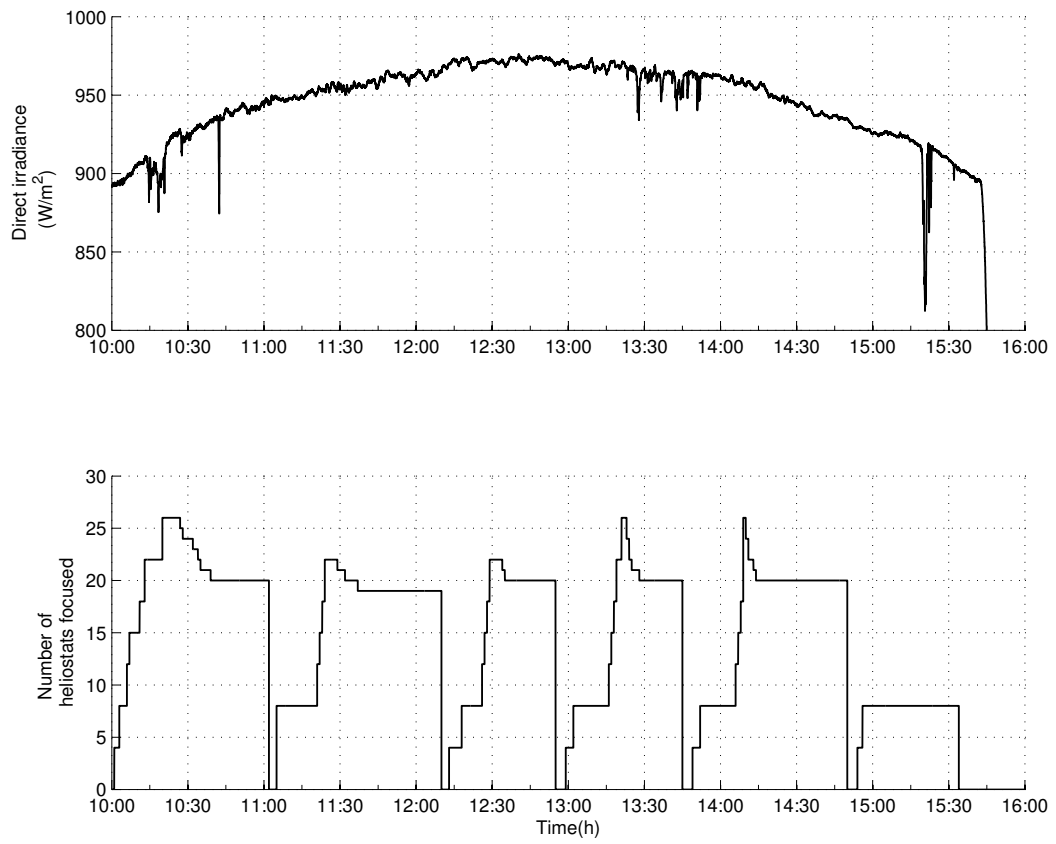


Figure 4: Inputs to the model to validate the thermal behaviour

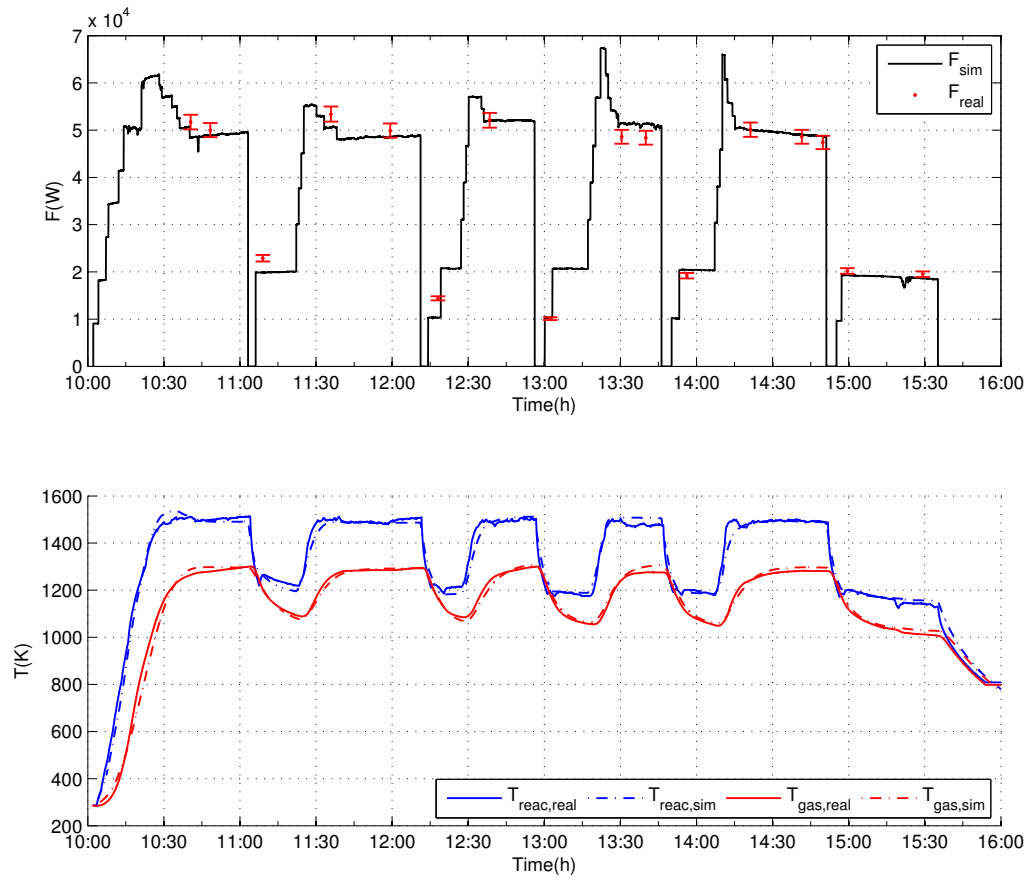


Figure 5: Validation of the thermal behavior of the model with experimental data

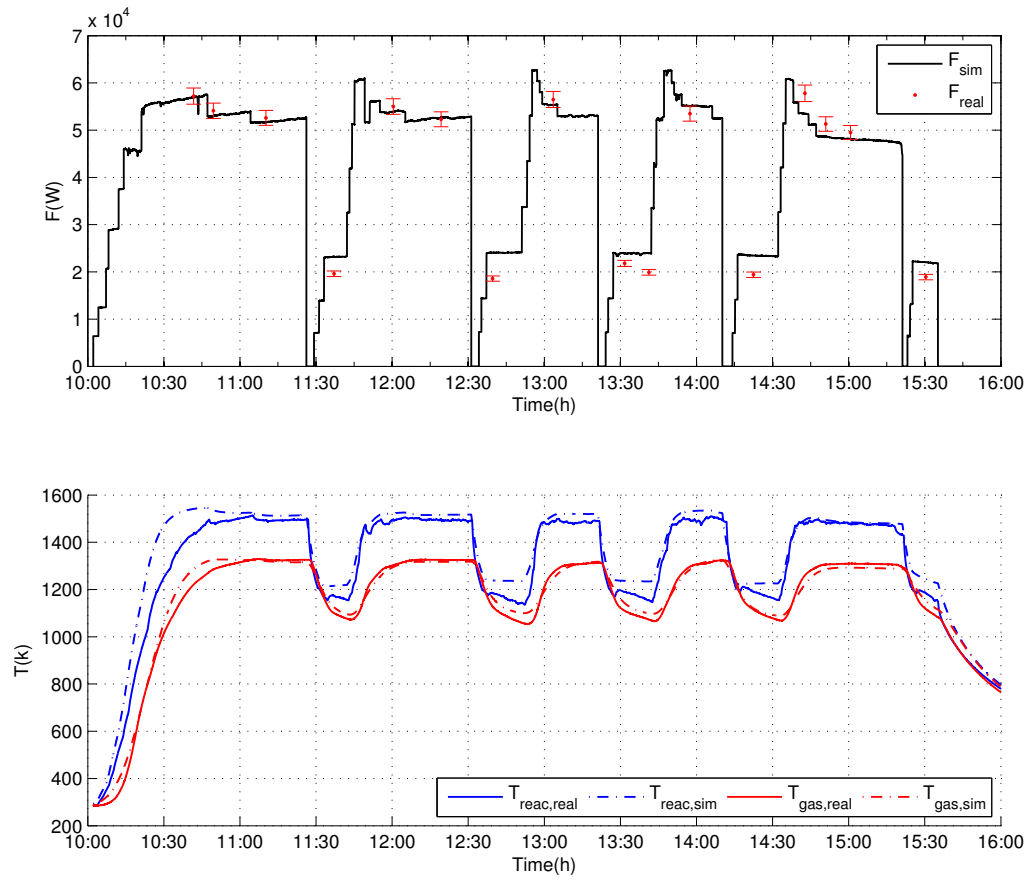


Figure 6: An example of the dependence between the two partial models

Table 1: Variables list

Name	Description	Units
$A$	Area	$\text{m}^2$
$C$	Specific heat capacity	$\text{J} \cdot \text{Kg}^{-1} \cdot \text{K}^{-1}$
$c_d$	Coefficient of discharge	1
$E_a$	Activation energy	J
$F$	Total concentration flux	W
$f$	One-heliostat concentration flux	W
$g$	Gravitational aceleration	$\text{m} \cdot \text{s}^{-2}$
$H_{conv}$	Convective heat transfer coefficient	$\text{J} \cdot \text{K}^{-1} \cdot \text{s}^{-1}$
$H_{rad}$	Radiative heat transfer coefficient	$\text{J} \cdot \text{K}^{-4} \cdot \text{s}^{-1}$
$h$	Specific enthalpy	$\text{J} \cdot \text{Kg}^{-1}$
$I$	Direct solar irradiance	$\text{W} \cdot \text{m}^{-2}$
$k_{gen}$	Generation rate constant	$\text{mol}^{-1} \cdot \text{s}^{-1}$
$k_{reg}$	Regeneration rate constant	$\text{s}^{-1}$
$m$	Mass	Kg
$n_t$	Total number of heliostats	1
$n$	Mole	mol
$p$	Pressure	Pa
$\mathbf{P}$	Position vector	(m, m, m)
$Q$	Heat	J
$R$	Reaction rate	$\text{mol} \cdot \text{s}^{-1}$
$s$	Slant range	m

$T$	Temperature	K
$t$	Target	m
$U$	Internal energy	J
$V$	Volume	$\text{m}^3$
$v$	Flow velocity	$\text{m} \cdot \text{s}^{-1}$
$z$	Spatial coordinate	m
$\alpha$	Angle	rad
$\beta$	Coefficient of slope, shading and blocking errors	1
$\gamma$	Coefficient of attenuation	1
$\rho$	Density	$\text{Kg} \cdot \text{m}^{-3}$

Table 2: Subscripts list

<b>Name</b>	<b>Description</b>
0	Initial
1	Reactor 1
2	Reactor 2
<i>a</i>	Acimuth
<i>conv</i>	Convective
<i>e</i>	Elevation
<i>env</i>	Environment
<i>h</i>	Heliostat
<i>helio</i>	Heliostat field
<i>i</i>	Incident
<i>in</i>	Inlet
<i>gas</i>	Gas
<i>gen</i>	Generation
<i>rad</i>	Radiative
<i>reac</i>	Reactor
<i>real</i>	Real
<i>reg</i>	Regeneration
<i>o</i>	Orifice
<i>out</i>	Outlet
<i>s</i>	Sun
<i>sim</i>	Simulated

$t$	Target
$x$	Spatial coordinate
$y$	Spatial coordinate
$z$	Spatial coordinate